

Exact zeros of the Loschmidt echo and quantum speed limit time for the dynamical quantum phase transition in finite-size systems

Bozhen Zhou,^{1,2} Yumeng Zeng,^{1,2} and Shu Chen^{1,2,3,*}

¹*Beijing National Laboratory for Condensed Matter Physics,*

Institute of Physics, Chinese Academy of Sciences, Beijing 100190, China

²*School of Physical Sciences, University of Chinese Academy of Sciences, Beijing 100049, China*

³*Yangtze River Delta Physics Research Center, Liyang, Jiangsu 213300, China*

(Dated: February 5, 2022)

We study exact zeros of Loschmidt echo and quantum speed limit time for dynamical quantum phase transition in finite size systems. Our results illustrate that exact zeros of Loschmidt echo exist even in finite size quantum systems when the postquench parameter takes some discrete values in regions with the corresponding equilibrium phase different from the initial phase. As the system size increases and tends to infinity, the discrete parameters distribute continuously in the parameter regions. We further analyze the time for the appearance of the first exact zero of Loschmidt echo which is known as the quantum speed limit time τ_{QSL} . We demonstrate that the maximal value of τ_{QSL} is proportional to L and approaches infinity in the thermodynamical limit, when we quench the initial non-critical state to the critical phase. We also calculate the minimal value of τ_{QSL} and find that its behavior is dependent on the phase of initial state.

I. INTRODUCTION

In recent years, the development of quantum simulation platforms, such as neutral atom arrays¹⁻⁴, stimulates the intensive studies on the nonequilibrium dynamics of quantum many-body systems. An interesting issue is the dynamical quantum phase transition (DQPT)⁵⁻³³, which describes dynamical quantum critical phenomena presented in quench dynamics of kinds of quantum systems with initial state chosen as the ground state of a given Hamiltonian and evolving under a sudden change of a Hamiltonian parameter. The DQPT is characterized by the emergence of zero points of Loschmidt echo (LE) at a series of critical times, where the LE is defined by $\mathcal{L}(t) = |\mathcal{G}(t)|^2$ with the Loschmidt amplitude given by

$$\mathcal{G}(t) = \langle \psi_i | e^{-iH_f t} | \psi_i \rangle. \quad (1)$$

Here $|\psi_i\rangle$ is the ground state of prequench Hamiltonian, H_f is the postquench Hamiltonian, and we have set $\hbar = 1$. The LE measures the overlap between initial quantum state and time-evolved state³⁴, which has wide application in various contexts ranging from the theory of quantum chaos³⁴⁻³⁶ and the Schwinger mechanism of particle production^{37,38}, to work distribution functions in the context of nonequilibrium fluctuation theorems^{39,40}. The existence of zero points of LE means the occurrence of nonanalytic behaviors of dynamical free energy, i.e., the rate function of LE given by $\lambda(t) = -\frac{1}{L} \ln \mathcal{L}(t)$, at these critical times. It has been shown that DQPT and the equilibrium quantum phase transition are closely related as the nonanalyticities in the rate function of LE occur for quenches crossing the static quantum phase transition point⁵⁻⁷, although a one-to-one correspondence between them does not always hold true^{9,10,41-43}. The relation between the long-time average of the LE and the ground state fidelity susceptibility⁴⁴⁻⁴⁸ was also unveiled recently⁴⁹.

In general, exact zeros of LE or nonanalyticities of dynamical free-energy only occur when the system size tends to infinity. This is very similar to Fisher zeros of the partition function in statistical physics⁵⁰. It is well known that the Fisher zeros in a finite size system do not lie on the real temperature axis, and exact zeros only emerge in the thermodynamic limit⁵⁰⁻⁵². Similarly, the exact zeros of LE in a finite size quantum system can only appear in the complex time plane. When the system size tends to infinity, the zeros approach to the real time axis for quenches crossing the quantum phase transition point⁵. Now a question arise here, one may ask whether exact zeros of LE can occur in real time axis for a finite size quantum system? If the answer is yes, it seems that there exists controversy with the known results and how to understand the seeming controversy?

Aiming to answer the above questions and deepen our understanding of DQPT in the finite size systems, we shall explore the exact zeros of LE by focusing on a well-known exact solvable model, i.e., the transverse field Ising model (TFIM), which is well studied and known to exhibit DQPT in the thermodynamic limit. The existence of exact solutions enable us to analytically derive the condition for the existence of exact zeros of LE in finite size systems. For a given initial state prepared as the ground state of pre-quench Hamiltonian, our results illustrate that exact zeros of LE exist even in finite size quantum systems when the post-quench parameter takes some discrete values. These discrete parameters are found to locate in regions with the corresponding equilibrium phase different from the initial phase. As the system size increases and tends to infinity, the discrete parameters distribute continuously in the parameter regions and thus are consistent with previous results.

Further, once we know the exact zeros of LE in finite size quantum systems, it is natural to explore the minimum time of an initial state evolving to its orthogonal state which corresponds to the time for the emergence of

the first exact zero of LE. The minimum time required for arriving an orthogonal quantum state is called quantum speed limit (QSL) time, denoted as τ_{QSL} . The QSL time gives fundamental limit on the time scale for how fast a quantum state evolves in real-time dynamics, and the lower bound of τ_{QSL} has been discussed in closed quantum systems⁵³⁻⁶³ and open quantum systems⁶⁴⁻⁶⁷. The discussion of QSL time can be traced back to the early time when Mandelstam and Tamm studied the time-energy uncertainty in non-relativistic quantum mechanics⁶⁸. The QSL time is also related to several interesting topics, such as quantum optimal control⁶⁹, quantum information⁷⁰ and quantum geometry⁷¹. In the framework of DQPT, the QSL time has been studied in a previous work⁷², which however, only concerns on the dynamics of the quantum critical state. As we shall clarify in this work, if the initial system is in the quantum critical state, no exact zeros of LE can be found and thus the connection of QSL time to the DQPT is still elusive. In this work, we shall unveil how the QSL time changes with quench parameters and explore the general connection between QSL time and DQPT by considering various situations with different quench parameters. We also pay particular attention to the maximum and minimum value of τ_{QSL} , as the maximum of τ_{QSL} is related to the quench dynamics close to critical point and the minimum of τ_{QSL} gives the important message for how fast the DQPT could happen. When the system size tends to infinity, we find that the maximum value of τ_{QSL} approaches infinity when the quench parameter approaches to the critical point, which is independent of the initial state. However, the behavior of the minimum value of τ_{QSL} is distinct if the initial state is chosen in different phase. We demonstrate that non-analytical behaviours appear in both the average of $\tau_{\text{min}}(L)$ and the variance of $\tau_{\text{min}}(L)$ when we change the prequench parameter across the static quantum phase transition point.

The article is organized as follows. In Sec. II, we study the quench dynamics in finite size systems of the transverse field Ising model and give exactly the relation for the occurrence of zeros of LE. The dynamical behavior quenched to the parameter region close to the critical point is also studied. In Sec. III, we study quantum speed limit time under different quench parameters and explore its connection to DQPT. A summary and outlook is given in Sec. IV.

II. EXACT ZEROS OF LOSCHMIDT ECHO IN FINITE SIZE SYSTEMS

We consider the one-dimensional (1D) TFIM described by the following Hamiltonian⁷³:

$$H = -J \sum_{j=1}^L \sigma_j^x \sigma_{j+1}^x - h \sum_{j=1}^L \sigma_j^z, \quad (2)$$

where J is the nearest-neighbor spin coupling, h is the external magnetic field along the z axis and the peri-

odical boundary condition $\sigma_{L+1}^x = \sigma_1^x$ is assumed. The three Pauli matrices are $\sigma_j^\alpha (\alpha = x, y, z)$, $j = 1, \dots, L$ with L denoting total number of lattice sites. The TFIM fulfills a duality relation^{74,75}: $UH(J, h)U^{-1} = JhH(1/J, 1/h)$. By using the Jordan-Wigner transformation, the even-parity and odd-parity of the TFIM with periodical boundary condition can be mapped to the anti-periodical Kitaev chain and periodical Kitaev chain, respectively^{76,77}. Then we can write the Hamiltonian in the fermion representation as

$$H = -J \sum_{j=1}^{L-1} \left(c_j^\dagger c_{j+1} + c_j^\dagger c_{j+1}^\dagger + \text{H.c.} \right) - 2h \sum_{j=1}^L c_j^\dagger c_j \pm J(c_L^\dagger c_1 + c_L^\dagger c_1^\dagger + \text{H.c.}), \quad (3)$$

where the plus sign or minus sign corresponds to the even-parity or odd-parity. For convenience, we take $J > 0$ in the following discussions so that the system is in the ferromagnetic phase when $|h/J| < 1$.

It is convenient to diagonalize the Hamiltonian (3) in the momentum space by using the Fourier transform $c_j^\dagger = \frac{1}{\sqrt{L}} \sum_k e^{ikj} c_k^\dagger$. Here values of k should be chosen in the set of $\mathcal{K}_{\text{PBC}} = \{k = \frac{2\pi m}{L} | m = -L/2 + 1, \dots, 0, \dots, L/2\}$ for periodical boundary condition (PBC) and $\mathcal{K}_{\text{aPBC}} = \{k = \pm \frac{\pi(2m-1)}{L} | m = 1, \dots, L/2\}$ for anti-periodical boundary condition (aPBC)^{77,78}. In the following discussion, we focus on the even site of lattice with even parity which is corresponding to aPBC. It should be noted that all terms of Hamiltonian come into pairs $(k, -k)$ for aPBC. Define the positive k values as $\mathcal{K}_{\text{aPBC}}^+ = \{k = \frac{\pi(2m-1)}{L} | m = 1, \dots, L/2\}$. Then the Hamiltonian in momentum space is

$$H = -2 \sum_{k \in \mathcal{K}_{\text{aPBC}}^+} \left[(J \cos k + h) (c_k^\dagger c_k - c_{-k} c_{-k}^\dagger) - (iJ \sin k c_k^\dagger c_{-k}^\dagger + \text{H.c.}) \right]. \quad (4)$$

By using the Bogoliubov transformation

$$\begin{aligned} \beta_k &= \cos \theta_k c_k + i \sin \theta_k c_{-k}^\dagger, \\ \beta_{-k}^\dagger &= i \sin \theta_k c_k + \cos \theta_k c_{-k}^\dagger, \end{aligned}$$

where $\frac{\epsilon_k}{E_k} = \cos 2\theta_k$ and $\frac{\zeta_k}{E_k} = \sin 2\theta_k$ with $\epsilon_k = -J \cos k - h$ and $\zeta_k = -J \sin k$, we arrive at a Hamiltonian given by^{73,76,77}

$$H = 2 \sum_{k \in \mathcal{K}_{\text{aPBC}}^+} \left(E_k \beta_k^\dagger \beta_k - E_k \beta_{-k} \beta_{-k}^\dagger \right), \quad (5)$$

where $E_k = \sqrt{\epsilon_k^2 + \zeta_k^2}$.

Then we consider the quench dynamics driven by the transverse field h which can be described by $h(t) =$

$h_i\Theta(-t) + h_f\Theta(t)$. The analytical formula of LE has the form

$$\mathcal{L}(t) = \prod_{k \in \mathcal{K}_{\text{aPBC}}^+} [1 - \sin^2(2\delta\theta_k) \sin^2(2E_{kf}t)], \quad (6)$$

where $\delta\theta_k = \theta_{kf} - \theta_{ki}$,

$$\theta_{ki} = \frac{1}{2} \arctan \frac{J \sin k}{J \cos k + h_i}$$

is the Bogoliubov angle of prequench Hamiltonian,

$$\theta_{kf} = \frac{1}{2} \arctan \frac{J \sin k}{J \cos k + h_f}$$

is the Bogoliubov angle of the postquench Hamiltonian, and E_{kf} is the energy of the postquench Hamiltonian. To ensure $\mathcal{L}(t) = 0$, we must have $\sin^2(2\delta\theta_k) = 1$, which gives rise to the following constraint relation

$$\frac{h_f}{J} = -\frac{J + h_i \cos k}{h_i + J \cos k}. \quad (7)$$

For a finite size system, the momentum k takes discrete values. Given the prequench parameter h_i , we can get a series of h_f determined by Eq. (7) for various k . When the postquench parameter takes these discrete values, we have $\mathcal{L}(t) = 0$ at

$$t = t_n^* = \frac{\pi}{2E_{kf}} \left(n + \frac{1}{2}\right), \quad (8)$$

with

$$E_{kf}/J = \sqrt{(\cos k + h_f/J)^2 + \sin^2 k}, \quad (9)$$

i.e., there exist exact zeros of LE as long as Eq. (7) is fulfilled. According to Eq. (7), if $h_i/J \in (-1, 1)$, the exact zeros of LE emerge only for $h_f/J \in (-\infty, -1) \cup (1, \infty)$. For the 1D transverse field Ising chain, we can prove that the Loschmidt echo fulfills the following dynamical duality relation

$$\mathcal{L}(\gamma_i, \gamma_f, t) = \mathcal{L}(\gamma_i^{-1}, \gamma_f^{-1}, \gamma_f t), \quad (10)$$

where $\gamma_i = h_i/J$ and $\gamma_f = h_f/J$ are the dimensionless parameters. Due to the existence of dynamical duality relation (see appendix for details), we only need to consider the case of $h_i/J \in (-1, 1)$ as the cases of $h_i/J \in (-\infty, -1)$ and $h_i/J \in (1, \infty)$ can be obtained by using the dynamical duality relation.

As displayed in Fig. 1(a) for the system with lattice size $L = 14$, for a given h_i/J , only $L/2$ discrete values of h_f/J satisfy Eq. (7). Continuously varying h_i/J leads to the formation of a series of curves in the parameter space spanned by h_i/J and h_f/J . When we increase the lattice size, the number of curves increases linearly and the distribution of curves becomes more and more dense, as shown in Fig. 1(b) for the system with $L = 400$.

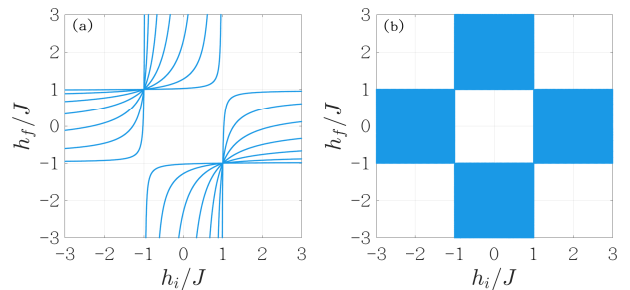


Figure 1. The combination of h_i/J and h_f/J which fulfill Eq. (7). (a) $L = 14$ and (b) $L = 400$.

To characterize the average distance between neighboring curves, we define the quantity $\bar{\Delta}$ as

$$\bar{\Delta} = \frac{1}{L-1} \sum_{k=\frac{1-L}{L}\pi}^{\frac{L-3}{L}\pi} \left| \frac{1}{J} \left[h_f \left(k + \frac{2\pi}{L}\right) - h_f(k) \right] \right|, \quad (11)$$

where $h_f(k)$ is the solution of Eq. (7) for a k mode. In the thermodynamic limit we can turn the sum into an integral and it can be found that $\bar{\Delta}$ is approximately equal to $4/L$ which approaches to 0 as $L \rightarrow \infty$. This is also confirmed by the numerical result as displayed in Fig. 2(a). Therefore the discrete values of h_f/J tend to distribute continuously in the thermodynamic limit, which is consistent with the general knowledge about the DQPT that zeros of LE appear when we quench the system across the critical point.

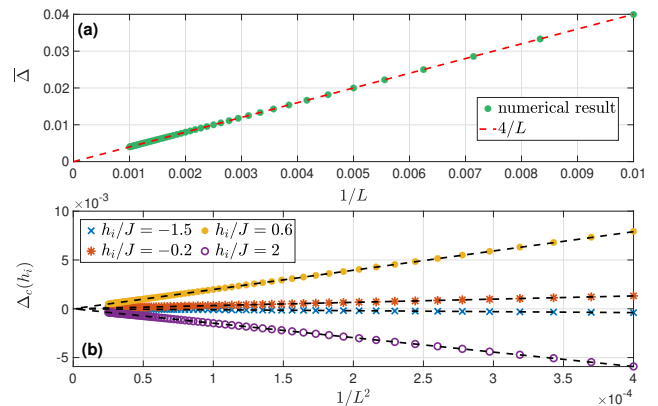


Figure 2. (a) Green dots are the numerical results of Eq. (11) for finite size systems. Red dashed line is the result in the large size limit $\bar{\Delta} \approx 4/L$. We set prequench parameter as $h_i/J = 1.5$. (b) The $\Delta_c(h_i)$ with respect to $1/L^2$ for different values of h_i/J . The discrete marks are the numerical results and the dashed lines are the results of Eq. (12).

If we quench the system to the critical point $h_f/J = 1$ (-1), from Eq. (7), we can see that no exact zeros of LE are available unless the initial state is prepared in the other critical point $h_i/J = -1$ (1). Interesting, if

we restrict $h_i/J \geq 0$ and $h_f/J \geq 0$, no exact zero of Loschmidt echo can be found if the value of h_i/J or h_f/J is in the interval $(-\cos \frac{L-1}{L}\pi, -\sec \frac{L-1}{L}\pi)$ for the finite size system. The interval $(-\cos \frac{L-1}{L}\pi, -\sec \frac{L-1}{L}\pi) \approx (1 - \frac{1}{2}(\frac{\pi}{L})^2, 1 + \frac{1}{2}(\frac{\pi}{L})^2)$ is around the critical point $h_c/J = 1$ and the boundary of the interval are reciprocal due to the existence of dynamical duality for the TFIM. Moreover, we can define a quantity $\Delta_c(h_i)$ which represents the shortest distance between $h_f/J = 1$ and the solutions of Eq. (7) for arbitrary value of h_i/J . The numerical result of $\Delta_c(h_i)$ is shown in Fig. 2(b) for $h_i/J = -1.5, -0.2, 0.6, 2$ represented by different marks. The approximate formula of $\Delta_c(h_i)$ for large L can be derived from Eq. (7), which reads as

$$\Delta_c(h_i) \approx \frac{\alpha(h_i)}{L^2}, \quad (12)$$

where $\alpha(h_i) = \frac{\pi^2(J+h_i)}{2(J-h_i)}$. The results of Eq. (12) for $h_i/J = -1.5, -0.2, 0.6, 2$ are shown in Fig. (2)(b) which are denoted by black dashed lines. So, if we quench the system from arbitrary value of h_i/J except -1 to h_f/J near the critical point, then there exists a region in which no exact zeros of LE are available for a finite size system. The width of this region is dependent on h_i/J and $\Delta_c(h_i) \rightarrow 0$ in the thermodynamic limit for any h_i/J . Together with the result of $\Delta \rightarrow 0$, we can see that exact zeros of LE would exist so long as we quench across the critical point for the infinite size system, in agreement with the previous work⁵ in the thermodynamic limit. The result of the shortest distance between $h_f/J = -1$ and the solutions of Eq. (7) for arbitrary value of h_i/J is similar to Eq. (12).

III. QUANTUM SPEED LIMIT TIME FOR DYNAMICAL QUANTUM PHASE TRANSITION

From the previous section, we know that there exist exact zeros of LE as we quench the ground state across the static phase transition point. It is known that the QSL time is the minimal time for the evolution of an initial state to its orthogonal state⁶⁰⁻⁶², and thus the time for the emergence of the first exact zero of LE gives the QSL time, i.e.,

$$\tau_{\text{QSL}} = \frac{\pi}{4E_{k_f}}. \quad (13)$$

According to Eq. (9), the QSL time is dependent on the values h_f/J .

As displayed in Fig. 3 for the system with $L = 22$, we show that a series of divergence points of rate function, corresponding to exact zeros of LE, appear in the real time axis. The QSL time corresponds to the first divergence point of rate function, which is labeled by black dashed line. To see the dependence of τ_{QSL} on h_f/J , we plot rate function versus Jt for all permitted $h_f/J > 0$

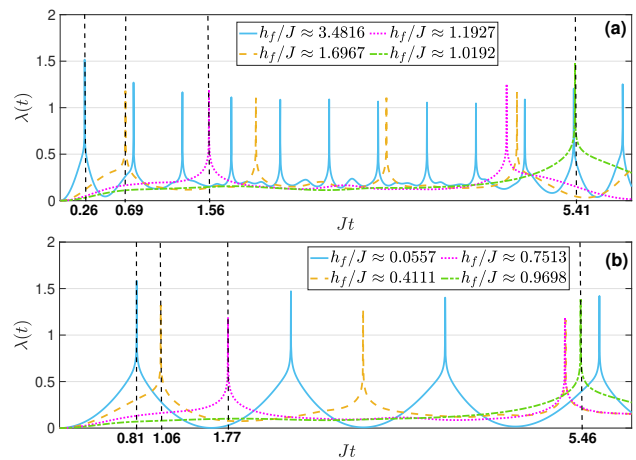


Figure 3. Rate function $\lambda(t)$ for $L = 22$. Black dashed lines guide the first time for the appearance of the exact zero of LE for every h_f/J . The prequench parameter is (a) $h_i/J = 0.3$ and (b) $h_i/J = 2$.

determined by Eq. (7). It can be observed from the Fig. 3(a) that the QSL time decreases with the increase in h_f/J , when we quench from the initial phase in the region of $0 < h_i/J < 1$ to the region of $h_f/J > 1$. On the other hand, when we quench from the region of $h_i/J > 1$ to $0 < h_f/J < 1$, the QSL time decreases with the decrease in h_f/J as shown in Fig. 3(b). Such an observation does not rely on the system size and can be obtained from Eq. (7) and Eq. (8). It follows that the QSL time increases as h_f/J approaches the critical point $h_f/J = 1$.

Particularly, we denote the maximal value of quantum speed limit time as $\tau_{max} = \max[\tau_{\text{QSL}}]$. It is found that τ_{max} is corresponding to the quench process with the postquench parameter closest to $h_c/J = 1$. From the analytical result Eq. (7) and the formula of E_{k_f} , it follows that $E_{k_f}/J \approx \frac{\pi}{L}$ is minima if $k = \frac{\pi}{L}$ or $k = \frac{L-1}{L}\pi$. According to Eq. (7), it should also be noted that the mode $k = \frac{\pi}{L}$ and $k = \frac{L-1}{L}\pi$ is corresponding to h_f/J closest to -1 and 1 for the finite size system, respectively. Then we have $\tau_{max} \approx L/(4J)$ which can be regarded as an upper bound of QSL time. As demonstrated in Fig. 4, we display the QSL time with respect to L for $h_i/J = 0.2, 0.6, 2, 10$ and h_f/J taken to be closest to -1 (Fig. 4(a)) and 1 (Fig. 4(b)), respectively. The red dashed lines in Fig. 4 guide the value of $\tau_{\text{QSL}} = L/(4J)$, indicating that τ_{max} increases linearly with the increase in the system size. In the thermodynamic limit, $k \rightarrow 0$ and $k \rightarrow \pi$ is corresponding to $h_f/J \rightarrow -1$ and $h_f/J \rightarrow 1$, respectively. When $L \rightarrow \infty$, we have $\tau_{max} \rightarrow \infty$ with $|h_f/J| \rightarrow 1$. This means that we can not observe the DQPT in a finite time if we quench the system from a non-critical phase to the critical phase with $|h_f/J| = 1$, i.e., no DQPT occurs in a finite time if we quench from a non-critical phase to the critical point due to the corresponding τ_{max} which is approaching infinity.

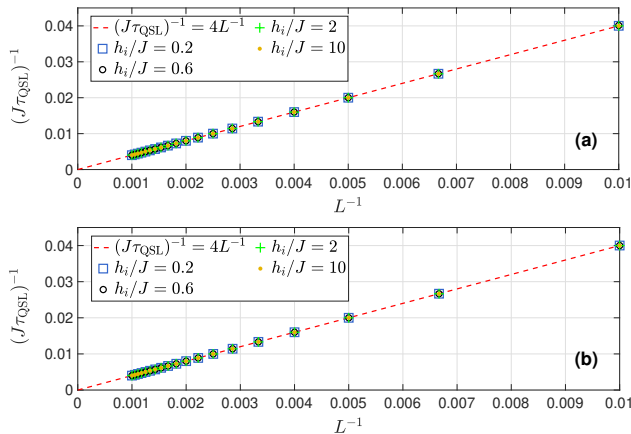


Figure 4. $(J\tau_{\text{QSL}})^{-1}$ versus L^{-1} for different prequench parameters. Here the postquench parameters fulfill Eq. (7) and are chosen to be closest to (a) $h_f/J = -1$ and (b) $h_f/J = 1$.

For any ground state of 1D TFIM, it is also interesting to ask how fast could the ground state achieve to its orthogonal state as we quench the parameter to the system? The answer of the question is given by the minimal value of QSL time denoted as $\tau_{\min} = \min[\tau_{\text{QSL}}]$. The closely related problem is Anderson's orthogonality catastrophe which demonstrates that a local perturbation can cause two many-body states to achieve orthogonality in the thermodynamic limit. And the connection between Anderson's orthogonality catastrophe and the QSL time in quantum quench dynamics has been discussed in recent work⁶². In Fig. 5, we demonstrate the behavior of $J\tau_{\min}$ for various prequench parameters h_i/J as the system size increases. It can be found that if the initial state lies in the paramagnetic phase [Fig. 5(a)], τ_{\min} would approach to some finite values as the system size increases. However, τ_{\min} would approach to zero if the initial state lies in the ferromagnetic phase [Fig. 5(b)].

To get a better understanding, now we discuss two limiting cases. One is the initial state chosen in the paramagnetic phase, i.e., the ground state of the prequench Hamiltonian with $h_i/J = \infty$. It can be seen that τ_{\min} is corresponding to the maximal value of $E_{kf}/J = \sqrt{(\cos k + h_f/J)^2 + \sin^2 k}$ with h_f/J fulfilling Eq. (7). For $h_i/J = \infty$, the maximal value of E_{kf} in the thermodynamic limit is $E_{kf}/J = 1$ corresponding to $k = \pi/2$, so we have $J\tau_{\min} = \frac{\pi}{4}$. We note that the exact zeros of LE in this limiting case have been discussed in Refs. [5,13,28]. And it can be observed in Fig. 5(a) for $h_i/J = 1000$, where the black dashed line guides the value of $\pi/4$. On the contrary, if we consider the prequench Hamiltonian lying in the ferromagnetic phase with $h_i/J = 0$. From Eq. (7), we have $h_f/J = -1/\cos k$, and it follows that the maximal value of E_{kf} is $E_{kf} = \infty$ corresponding to $k = \pi/2$, which means $\tau_{\min} = 0$ in the

thermodynamic limit. For the finite size system, k can be exactly equal to $\frac{\pi}{2}$ if $\text{mod}(L, 4) = 2$, so we have $\tau_{\min} = 0$. Otherwise, $k = \frac{\pi}{2} + \frac{\pi}{L}$ is the mode closest to $\frac{\pi}{2}$ for $\text{mod}(L, 4) = 0$. In this case, we have $h_f/J \approx \frac{L}{\pi}$ for $L \rightarrow \infty$ and the maximal value of $E_{kf}/J \approx \frac{L}{\pi}$ with $k = \frac{\pi}{2} + \frac{\pi}{L}$. Then we have $J\tau_{\text{QSL}} \approx \frac{\pi^2}{4L}$ which is illustrated in Fig. 5(b) by the green solid line and it is shown that the asymptotic behavior of τ_{QSL} is captured by the line of $\frac{\pi^2}{4L}$ for $|h_i/J| < 1$.

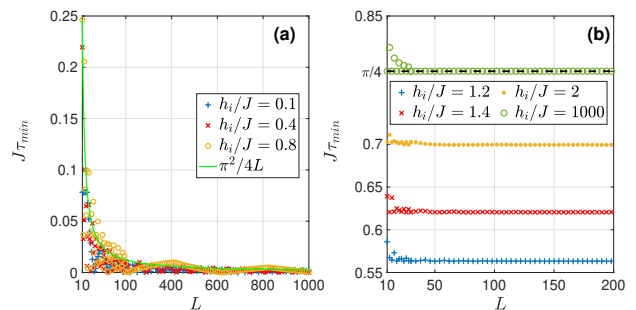


Figure 5. $J\tau_{\min}$ versus system size L . The prequench parameter is (a) $|h_i/J| > 1$ and (b) $|h_i/J| < 1$.

It is known that the lower bound of QSL time can be given by Mandelstam–Tamm bound τ_{MT} ^{54,56,68}:

$$\tau_{\text{QSL}} \geq \tau_{\text{MT}} \equiv \frac{\pi}{2\Delta E}, \quad (14)$$

where $(\Delta E)^2 = \langle \psi_i | H_f^2 | \psi_i \rangle - (\langle \psi_i | H_f | \psi_i \rangle)^2$ with H_f denotes the postquench Hamiltonian. Next, we consider the two cases discussed above. For the case with paramagnetic initial state $|\psi_i\rangle = \otimes_{j=1}^L |\uparrow\rangle_j$ and the postquench Hamiltonian $H_f = -J \sum_{j=1}^L \sigma_j^x \sigma_{j+1}^x$ with $h_f/J = 0$, we have $\Delta E = J\sqrt{L}$ due to $\langle \psi_i | H_f^2 | \psi_i \rangle = J^2 L$ and $\langle \psi_i | H_f | \psi_i \rangle = 0$. So the MT bound is $\tau_{\text{MT}} \rightarrow 0$ in the thermodynamical limit. For the other case with the ferromagnetic initial state $|\psi_i\rangle = \otimes_{j=1}^L |\rightarrow\rangle_j$ (or $|\psi_i\rangle = \otimes_{j=1}^L |\leftarrow\rangle_j$) and $H_f = -h_f \sum_{j=1}^L \sigma_j^z$ with $h_f/J \rightarrow \infty$, we have $\Delta E \rightarrow \infty$ and $\tau_{\text{MT}} \rightarrow 0$. It can be seen that the MT bound of QSL time is equal to zero for both two cases. In comparison with our exact result of τ_{QSL} , it can be found that the MT bound τ_{MT} is tight if the prequench Hamiltonian lies in the ferromagnetic phase.

To see clearly how $\tau_{\min}(L)$ changes with h_i/J , we can calculate the mean value of $\tau_{\min}(L)$ numerically from L_{\min} to L_{\max} and denote it as:

$$\bar{\tau}_{\min} = \frac{1}{L_{\max} - L_{\min}} \sum_{L=L_{\min}}^{L_{\max}} \tau_{\min}(L). \quad (15)$$

Meanwhile, we can also calculate the variance of $\tau_{\min}(L)$ defined by:

$$\sigma_{\tau_{\min}}^2 = \frac{1}{L_{\max} - L_{\min}} \sum_{L=L_{\min}}^{L_{\max}} [\tau_{\min}^2(L) - \bar{\tau}_{\min}^2]. \quad (16)$$

We count from $L_{min} = 10$ to $L_{max} = 10000$ and show the numerical results of $J\bar{\tau}_{min}$ and $J^2\sigma_{\tau_{min}}^2$ with respect to prequench parameter h_i/J in Figs. 6(a) and 6(b), respectively. It can be observed that both $\bar{\tau}_{min}$ and $\sigma_{\tau_{min}}^2$ have an abrupt change at $h_i/J = 1$ which corresponds to the static quantum phase transition point in the thermodynamic limit. The fluctuation of energy can be evidenced in $\sigma_{\tau_{min}}^2$ (Fig. 6(b)) which remains a nonzero value as $|h_i/J| < 1$ and diverges as $|h_i/J|$ approaches 1. The non-analytical behaviours appearing in the change of prequench parameter across the static quantum phase transition point indicates that clearly the minima of QSL time relies on the choice of initial states.

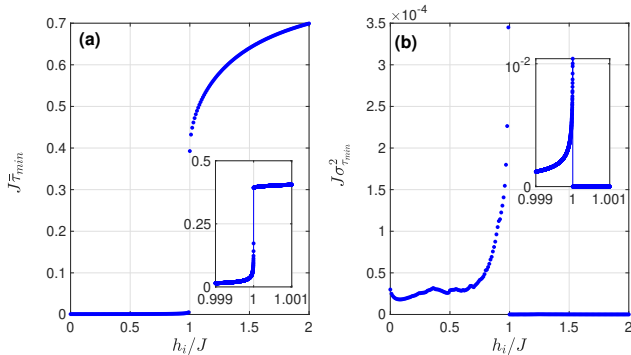


Figure 6. (a) $J\bar{\tau}_{min}$ with respect to h_i/J ; (b) $J^2\sigma_{\tau_{min}}^2$ with respect to h_i/J . Here we count the size of system from $L_{min} = 10$ to $L_{max} = 10000$.

IV. SUMMARY AND OUTLOOK

In summary, we have analytically calculated the exact zeros of the LE for the 1D TFIM and shown that there exist exact zeros of LE even for the finite size quantum system when the post-quench parameter takes some discrete values. As the system size tends to infinity, the discrete parameters distribute continuously in the parameter regions with the corresponding equilibrium phase different from the initial phase, which is in agreement with previous work in the thermodynamic limit. We also unveil that no exact zeros of LE are available if we quench the system to (or from) the critical point. For the finite size systems of 1D TFIM, we have unveiled how the QSL time changes with quench parameters and studied the behaviors of the maximum and minimum values of the QSL time. From our analytical result in the thermodynamic limit, it is shown that no DQPT occurs in a finite time if we quench from a non-critical phase to the critical point due to that the corresponding τ_{max} is approaching infinity. We have also illustrated the existence of non-analytical behaviors in both the average of $\tau_{min}(L)$ and the variance of $\tau_{min}(L)$ when we change the parameter of prequench Hamiltonian across the underlying static critical point.

Our work provides a firm theoretical ground for understanding why and how the DQPT occurs with the increase of system sizes and the peculiar dynamical behavior near the critical point, which paves the way for experimental investigations of DQPT for small size systems. According to our theoretical finding, we can always find exact zeros of LE by tuning the quench parameter to a series of discrete fine-tuning points for the finite size system which supports DQPT in the thermodynamical limit. At these fine-tuning points, the divergence of the corresponding rate function can be observed in some critical times. The number of fine-tuning points increases linearly with the increase of lattice size. By recording the critical times for the emergence of exact zeros of LE, one can also experimentally study the behaviors of quantum speed limit time and explore its connection to the DQPT.

ACKNOWLEDGMENTS

This work is supported by National Key Research and Development Program of China (2016YFA0300600), NSFC under Grants No.11974413 and the Strategic Priority Research Program of Chinese Academy of Sciences under Grant No. XDB33000000.

Appendix A: The dynamical duality relation of the Loschmidt echo

Consider the quench dynamics of the quantum TFIM by suddenly switching the transverse field from the prequench parameter h_i to the postquench parameter h_f . The Loschmidt echo can be represented as

$$\mathcal{L}(\gamma_i, \gamma_f, t) = \prod_k \mathcal{L}_k(\gamma_i, \gamma_f, t), \quad (\text{A1})$$

where $\gamma_i = h_i/J$ and $\gamma_f = h_f/J$ are the dimensionless parameters and the k -component of the Loschmidt echo is

$$\mathcal{L}_k(\gamma_i, \gamma_f, t) = 1 - \sin^2(2\delta\theta_k) \sin^2(2E_{kf}t). \quad (\text{A2})$$

Here we have

$$\begin{aligned} & \sin^2(2\delta\theta_k) \\ &= \left(\frac{\zeta_f}{E_f} \frac{\epsilon_i}{E_i} - \frac{\epsilon_f}{E_f} \frac{\zeta_i}{E_i} \right)^2 \\ &= \frac{(\zeta_f \epsilon_i - \epsilon_f \zeta_i)^2}{(\epsilon_i^2 + \zeta_i^2)(\epsilon_f^2 + \zeta_f^2)} \\ &= \frac{(\gamma_i - \gamma_f)^2 \sin^2 k}{(1 + 2\gamma_i \cos k + \gamma_i^2)(1 + 2\gamma_f \cos k + \gamma_f^2)}, \end{aligned}$$

and

$$\sin^2(2E_{kf}t) = \sin^2\left(2J_f t \sqrt{1 + 2\gamma_f \cos k + \gamma_f^2}\right)$$

Now we consider the case with the prequench and postquench dimensionless parameters being $1/\gamma_i$ and $1/\gamma_f$, respectively. The k -component of Loschmidt echo of the corresponding model can be written as

$$\mathcal{L}_k\left(\frac{1}{\gamma_i}, \frac{1}{\gamma_f}, t\right) = 1 - \sin^2\left(2\delta\tilde{\theta}_k\right) \sin^2\left(2\tilde{E}_{kf}t\right), \quad (\text{A3})$$

with

$$\begin{aligned} & \sin^2\left(2\delta\tilde{\theta}_k\right) \\ &= \frac{\left(\gamma_i^{-1} - \gamma_f^{-1}\right)^2 \sin^2 k}{\left(1 + 2\gamma_i^{-1} \cos k + \gamma_i^{-2}\right) \left(1 + 2\gamma_f^{-1} \cos k + \gamma_f^{-2}\right)} \\ &= \frac{\left(\gamma_i - \gamma_f\right)^2 \sin^2 k}{\left(\gamma_i^2 + 2\gamma_i \cos k + 1\right) \left(\gamma_f^2 + 2\gamma_f \cos k + 1\right)} \\ &= \sin^2\left(2\delta\theta_k\right), \end{aligned}$$

and

$$\sin^2\left(2\tilde{E}_{kf}t\right) = \sin^2\left(2E_{kf}\gamma_f^{-1}t\right)$$

where $\tilde{E}_{kf} \equiv E_{kf}(1/\gamma_f)$ and we have used the dual relation of eigenvalues $E_{kf}(\gamma_f) = \gamma_f E_{kf}(1/\gamma_f)$.

Then we can observe that

$$\mathcal{L}_k(\gamma_i, \gamma_f, t) = \mathcal{L}_k(\gamma_i^{-1}, \gamma_f^{-1}, \gamma_f t). \quad (\text{A4})$$

which gives rise to the dynamical dual relation Eq. (10) directly.

Appendix B: The case under periodical boundary condition

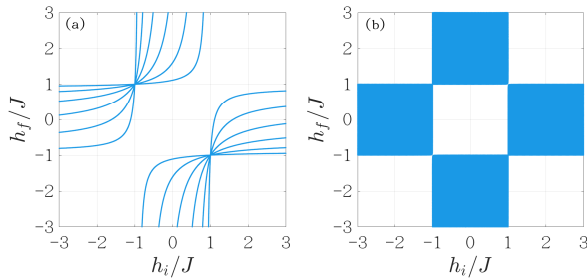


Figure 7. The combination of h_i/J and h_f/J which fulfill Eq. (7) under the PBC for odd parity space. (a) $L = 14$ and (b) $L = 400$.

In the main text, we have taken the anti-periodical boundary condition. In this appendix, we consider the odd parity of the 1D TFIM which corresponds to the periodical boundary condition of Hamiltonian Eq. (3). The formulas for determining exact zeros of LE in the main text do not change, and the constraint relation of quench parameter is the same as the Eq. (7). However, the values of k under PBC should be chosen in the set of $\mathcal{K}_{\text{PBC}} = \{k = \frac{2\pi m}{L} | m = -L/2 + 1, \dots, 0, \dots, L/2\}$. Here the modes corresponding to $k = 0$ and $k = \pi$ should be removed due to $\sin^2(2\delta\theta_k) = 0$ and thus $\mathcal{L}_k = 1$ for $k = 0$ or $k = \pi$. Therefore, under the PBC, for a given h_i/J , only $L/2 - 1$ discrete values of h_f/J satisfy Eq. (7) corresponding to $k = \frac{2\pi}{L}, \dots, \frac{2\pi(L/2-1)}{L}$. We display the result of Eq. (7) in Fig. 7(a) and (b) for $L = 14$ and $L = 400$ under the PBC, respectively, in contrast to Fig. 1 for the same system under the aPBC. When the system size tends to infinity, the discrete values of h_f/J tend to distribute continuously, and therefore our conclusions do not rely on boundary conditions in the thermodynamical limit.

* Corresponding author: schen@iphy.ac.cn

¹ H. Bernien, S. Schwartz, A. Keesling, H. Levine, A. Om-

ran, H. Pichler, S. Choi, A. S. Zibrov, M. Endres, M. Greiner et al., Probing many-body dynamics on a 51-atom

- quantum simulator, *Nature (London)* **551**, 579 (2017).
- ² A. Omran, H. Levine, A. Keesling, G. Semeghini, T. T. Wang, S. Ebadi, H. Bernien, A. S. Zibrov, H. Pichler, S. Choi et al., Generation and manipulation of Schrödinger cat states in Rydberg atom arrays, *Science* **365**, 570 (2019).
 - ³ D. Bluvstein, A. Omran, H. Levine, A. Keesling, G. Semeghini, S. Ebadi, T. T. Wang, A. A. Michailidis, N. Maskara, W. W. Ho et al., Controlling many-body dynamics with driven quantum scars in Rydberg atom arrays, *Science* **371**, 1355 (2021).
 - ⁴ S. Ebadi, T. T. Wang, H. Levine, A. Keesling, G. Semeghini, A. Omran, D. Bluvstein, R. Samajdar, H. Pichler, Wen Wei Ho et al., Quantum phases of matter on a 256-Atom programmable quantum simulator, *Nature (London)* **595**, 227 (2021).
 - ⁵ M. Heyl, A. Polkovnikov, S. Kehrein, Dynamical quantum phase transitions in the transverse-field Ising model, *Phys. Rev. Lett.* **110**, 135704 (2013).
 - ⁶ C. Karrasch and D. Schuricht, Dynamical phase transitions after quenches in nonintegrable models, *Phys. Rev. B* **87**, 195104 (2013).
 - ⁷ J. M. Hickey, S. Genway, and J. P. Garrahan, Dynamical phase transitions, time-integrated observables, and geometry of states, *Phys. Rev. B* **89**, 054301 (2014).
 - ⁸ E. Canovi, P. Werner, and M. Eckstein, First-order dynamical phase transitions, *Phys. Rev. Lett.* **113**, 265702 (2014).
 - ⁹ F. Andraschko and J. Sirker, Dynamical quantum phase transitions and the Loschmidt echo: A transfer matrix approach, *Phys. Rev. B* **89**, 125120 (2014).
 - ¹⁰ M. Schmitt and S. Kehrein, Dynamical quantum phase transitions in the Kitaev honeycomb model, *Phys. Rev. B* **92**, 075114 (2015).
 - ¹¹ M. Marcuzzi, E. Levi, S. Diehl, J. P. Garrahan, and I. Lesanovsky, Universal nonequilibrium properties of dissipative Rydberg gases, *Phys. Rev. Lett.* **113**, 210401 (2014).
 - ¹² M. Heyl, Dynamical Quantum phase transitions in systems with broken-symmetry phases, *Phys. Rev. Lett.* **113**, 205701 (2014).
 - ¹³ M. Heyl, Scaling and universality at dynamical quantum phase transitions, *Phys. Rev. Lett.* **115**, 140602 (2015).
 - ¹⁴ S. Vajna and B. Dóra, Topological classification of dynamical phase transitions, *Phys. Rev. B* **91**, 155127 (2015).
 - ¹⁵ N. O. Abeling and S. Kehrein, Quantum quench dynamics in the transverse field Ising model at nonzero temperatures, *Phys. Rev. B* **93**, 104302 (2016).
 - ¹⁶ J. C. Budich and M. Heyl, Dynamical topological order parameters far from equilibrium, *Phys. Rev. B* **93**, 085416 (2016).
 - ¹⁷ A. A. Zvyagin, Dynamical quantum phase transitions (Review Article), *Fiz. Nizk. Temp. (Kiev)* **42**, 1240 (2016) [*Low Temp. Phys.* **42**, 971 (2016)].
 - ¹⁸ M. Heyl, Dynamical quantum phase transitions: a review, *Rep. Prog. Phys.* **81**, 054001 (2018).
 - ¹⁹ C. Yang, Y. Wang, P. Wang, X. Gao and S. Chen, Dynamical signature of localization-delocalization transition in a one-dimensional incommensurate lattice, *Phys. Rev. B* **95**, 184201 (2017).
 - ²⁰ M. Heyl, F. Pollmann, and B. Dóra, Detecting equilibrium and dynamical quantum phase transitions in Ising chains via out-of-time-ordered correlators, *Phys. Rev. Lett.* **121**, 016801 (2018).
 - ²¹ C. Yang, L. Li and S. Chen, Dynamical topological invariant after a quantum quench, *Phys. Rev. B* **97**, 060304(R) (2018).
 - ²² B. Mera, C. Vlachou, N. Paunković, V. R. Vieira, and O. Viyuela, Dynamical phase transitions at finite temperature from fidelity and interferometric Loschmidt echo induced metrics, *Phys. Rev. B* **97**, 094110 (2018).
 - ²³ P. Jurcevic, H. Shen, P. Hauke, C. Maier, T. Brydges, C. Hempel, B. P. Lanyon, M. Heyl, R. Blatt, and C. F. Roos, Direct observation of dynamical quantum phase transitions in an interacting many-body system, *Phys. Rev. Lett.* **119**, 080501 (2017).
 - ²⁴ X.-Y. Guo, C. Yang, Y. Zeng, Y. Peng, H.-K. Li, H. Deng, Y.-R. Jin, S. Chen, D. Zheng, and H. Fan, Observation of a dynamical quantum phase transition by a superconducting qubit simulation, *Phys. Rev. Applied* **11**, 044080 (2019).
 - ²⁵ N. Fläschner, D. Vogel, M. Tarnowski, B. S. Rem, D.-S. Lühmann, M. Heyl, J. C. Budich, L. Mathey, K. Sengstock, and C. Weitenberg, Observation of dynamical vortices after quenches in a system with topology, *Nat. Phys.* **14**, 265 (2018).
 - ²⁶ K. Wang, X. Qiu, L. Xiao, X. Zhan, Z. Bian, W. Yi, and P. Xue, Simulating dynamic quantum phase transitions in photonic quantum walks, *Phys. Rev. Lett.* **122**, 020501 (2019).
 - ²⁷ X. Nie, B.-B. Wei, X. Chen, Z. Zhang, X. Zhao, C. Qiu, Y. Tian, Y. Ji, T. Xin, D. Lu, and J. Li, Experimental Observation of Equilibrium and Dynamical Quantum Phase Transitions via Out-of-Time-Ordered Correlators, *Phys. Rev. Lett.* **124**, 250601 (2020).
 - ²⁸ G. Sun and B.-B. Wei, Dynamical quantum phase transitions in a spin chain with deconfined quantum critical points, *Phys. Rev. B* **102**, 094302 (2020).
 - ²⁹ R. Jafari, H. Johannesson, A. Langari, M. A. Martin-Delgado, Quench dynamics and zero-energy modes: The case of the Creutz model, *Phys. Rev. B* **99**, 054302 (2019).
 - ³⁰ J. C. Halimeh and V. Zauner-Stauber, Dynamical phase diagram of spin chains with long-range interactions, *Phys. Rev. B* **96**, 134427 (2017).
 - ³¹ S. P. Pedersen and N. T. Zinner, Lattice gauge theory and dynamical quantum phase transitions using noisy intermediate-scale quantum devices, *Phys. Rev. B* **103**, 235103 (2021).
 - ³² I. Homrighausen, N. O. Abeling, V. Zauner-Stauber, and J. C. Halimeh, Anomalous dynamical phase in quantum spin chains with long-range interactions, *Phys. Rev. B* **96**, 104436 (2017).
 - ³³ R. Jafari and A. Akbari, Floquet dynamical phase transition and entanglement spectrum, *Phys. Rev. A* **103**, 012204 (2021).
 - ³⁴ T. Gorin, T. Prosen, T. H. Seligman, and M. Znidaric, Dynamics of Loschmidt echoes and fidelity decay, *Phys. Rep.* **435**, 33 (2006).
 - ³⁵ A. Peres, Stability of quantum motion in chaotic and regular systems, *Phys. Rev. A* **30**, 1610 (1984).
 - ³⁶ R. A. Jalabert and H. M. Pastawski, Environment-independent decoherence rate in classically chaotic systems, *Phys. Rev. Lett.* **86**, 2490 (2001).
 - ³⁷ A. E. Martinez, A. C. Muschik, P. Schindler, D. Nigg, A. Erhard, M. Heyl, P. Hauke, M. Dalmonte, T. Monz, P. Zoller and R. Blatt, Real-time dynamics of lattice gauge theories with a few-qubit quantum computer, *Nature* **534**, 516 (2016).
 - ³⁸ J. Schwinger, On gauge invariance and vacuum polariza-

- tion, Phys. Rev. **82**, 664 (1951).
- ³⁹ P. Talkner, E. Lutz and P. Hänggi, Fluctuation theorems: Work is not an observable, Phys. Rev. E **75**, 050102 (2007).
- ⁴⁰ T. Palmai, Edge exponents in work statistics out of equilibrium and dynamical phase transitions from scattering theory in one-dimensional gapped systems, Phys. Rev. B **92**, 235433 (2015).
- ⁴¹ S. Vajna and B. Dora, Disentangling dynamical phase transitions from equilibrium phase transitions, Phys. Rev. B **89**, 161105(R) (2014).
- ⁴² S. Sharma, S. Suzuki, and A. Dutta, Quenches and dynamical phase transitions in a nonintegrable quantum Ising model, Phys. Rev. B **92**, 104306 (2015).
- ⁴³ R. Jafari, Dynamical quantum phase transition and quasi particle excitation, Sci. Rep. **9**, 2871 (2019).
- ⁴⁴ P. Zanardi and N. Paunković, Ground state overlap and quantum phase transitions, Phys. Rev. E **74**, 031123 (2006).
- ⁴⁵ W. L. You, Y. W. Li, and S. J. Gu, Fidelity, dynamic structure factor, and susceptibility in critical phenomena, Phys. Rev. E **76**, 022101 (2007).
- ⁴⁶ S. Chen, L. Wang, Y. Hao, and Y. Wang, Intrinsic relation between ground-state fidelity and the characterization of a quantum phase transition, Phys. Rev. A **77**, 032111 (2008).
- ⁴⁷ S. Chen, L. Wang, S. J. Gu, and Y. Wang, Fidelity and quantum phase transition for the Heisenberg chain with next-nearest-neighbor interaction, Phys. Rev. E **76**, 061108 (2007).
- ⁴⁸ H. Q. Zhou and J. P. Barjaktarevic, Fidelity and quantum phase transitions, J. Phys. A **41**, 412001 (2008).
- ⁴⁹ B. Zhou, C. Yang, and S. Chen, Signature of a nonequilibrium quantum phase transition in the long-time average of the Loschmidt echo, Phys. Rev. B **100**, 184313 (2019).
- ⁵⁰ M. E. Fisher, in *Boulder Lectures in Theoretical Physics* (University of Colorado, Boulder, 1965), Vol. 7.
- ⁵¹ C. N. Yang and T. D. Lee, Statistical theory of equations of state and phase transitions. I. Theory of condensation, Phys. Rev. **87**, 404 (1952).
- ⁵² W. van Saarloos and D. Kurtze, Location of zeros in the complex temperature plane: absence of Lee-Yang theorem, J. Phys. A **17**, 1301 (1984).
- ⁵³ G. N. Fleming, A unitarity bound on the evolution of non-stationary states, Nuovo Cimento A **16**, 232 (1973).
- ⁵⁴ K. Bhattacharyya, Quantum decay and the Mandelstam-Tamm-energy inequality, J. Phys. A: Math. Gen. **16**, 2993 (1983).
- ⁵⁵ J. Anandan and Y. Aharonov, Geometry of quantum evolution, Phys. Rev. Lett. **65**, 1697 (1990).
- ⁵⁶ Lev Vaidman, Minimum time for the evolution to an orthogonal quantum state, Am. J. Phys. **60**, 182 (1992).
- ⁵⁷ J. Uffink, The rate of evolution of a quantum state, Am. J. Phys. **61**, 935 (1993).
- ⁵⁸ P. Pfeifer, How fast can a quantum state change with time?, Phys. Rev. Lett. **70**, 3365 (1993).
- ⁵⁹ N. Margolus and L. B. Levitin, The maximum speed of dynamical evolution, Physica (Amsterdam) **120D**, 188 (1998).
- ⁶⁰ V. Giovannetti, S. Lloyd, and L. Maccone, Quantum limits to dynamical evolution, Phys. Rev. A **67**, 052109 (2003).
- ⁶¹ L. B. Levitin and T. Toffoli, Fundamental limit on the rate of quantum dynamics: The unified bound is tight, Phys. Rev. Lett. **103**, 160502 (2009).
- ⁶² T. Fogarty, S. Deffner, T. Busch and S. Campbell, Orthogonality catastrophe as a consequence of the quantum speed limit, Phys. Rev. Lett. **124**, 110604 (2020).
- ⁶³ N. Il'in and O. Lychkovskiy, Quantum speed limit for thermal states, Phys. Rev. A **103**, 062204 (2021).
- ⁶⁴ A. del Campo, I. L. Egusquiza, M. B. Plenio, and S. F. Huelga, Quantum speed limits in open system dynamics, Phys. Rev. Lett. **110**, 050403 (2013).
- ⁶⁵ S. Deffner and E. Lutz, Quantum Speed Limit for Non-Markovian Dynamics, Phys. Rev. Lett. **111**, 010402 (2013).
- ⁶⁶ N. Mirkin, F. Toscano and D.A. Wisniacki, Quantum-speed-limit bounds in an open quantum evolution, Phys. Rev. A **94**, 052125 (2016).
- ⁶⁷ T. V. Vu and Y. Hasegawa, Geometrical Bounds of the Irreversibility in Markovian Systems, Phys. Rev. Lett. **126**, 010601 (2021).
- ⁶⁸ L. Mandelstam and I. Tamm, The uncertainty relation between energy and time in nonrelativistic quantum mechanics, J. Phys. (Moscow) **9**, 249 (1945).
- ⁶⁹ S. van Frank, M. Bonneau, J. Schmiedmayer, S. Hild, C. Gross, M. Cheneau, I. Bloch, T. Pichler, A. Negretti, T. Calarco and S. Montangero, Optimal control of complex atomic quantum systems, Sci. Rep. **6**, 34187 (2016).
- ⁷⁰ Sebastian Deffner, Quantum speed limits and the maximal rate of information production, Phys. Rev. Research **2**, 013161 (2020)
- ⁷¹ D. P. Pires, M. Cianciaruso, L. C. Céleri, G. Adesso, and D. O. Soares-Pinto, Generalized Geometric Quantum Speed Limits, Phys. Rev. X **6**, 021031 (2016).
- ⁷² M. Heyl, Quenching a quantum critical state by the order parameter: Dynamical quantum phase transitions and quantum speed limits, Phys. Rev. B **95**, 060504(R) (2017).
- ⁷³ P. Pfeuty, The one-dimensional Ising model with a transverse field, Ann. Phys. (N.Y.) **57**, 79 (1970).
- ⁷⁴ E. Fradkin and L. Susskind, Order and disorder in gauge systems and magnets, Phys. Rev. D **17**, 2637 (1978).
- ⁷⁵ L. Zhang, Universal thermodynamic signature of self-dual quantum critical points, Phys. Rev. Lett. **123**, 230601 (2019).
- ⁷⁶ E. Lieb, T. Schultz, and D. Mattis, Two soluble models of an antiferromagnetic chain, Ann. Phys. (NY) **16**, 407 (1961).
- ⁷⁷ G. B. Mbeng, A. Russomanno, G. E. Santoro, The quantum Ising chain for beginners, arXiv:2009.09208v1.
- ⁷⁸ B. Damski and M. M Rams, Exact results for fidelity susceptibility of the quantum Ising model: the interplay between parity, system size, and magnetic field, J. Phys. A: Math. Theor. **47**, 025303 (2014).